International Journal of Heat and Mass Transfer 100 (2016) 938–948

Contents lists available at ScienceDirect

International Journal of Heat and Mass Transfer

journal homepage: www.elsevier.com/locate/ijhmt

Two-dimensional mesoscale simulations of saturated pool boiling from rough surfaces. Part II: Bubble interactions above multi-cavities

Shuai Gong, Ping Cheng *

MOE Key Laboratory for Power Machinery and Engineering, School of Mechanical Engineering, Shanghai Jiao Tong University, Shanghai 200240, PR China

ARTICLE INFO

Article history:
Received 12 January 2016
Received in revised form 22 April 2016
Accepted 23 April 2016
Available online 12 May 2016

Keywords:
Pool boiling
Lattice Boltzmann method
Cavity
Bubble interaction
Boiling curve

ABSTRACT

Bubble interactions and their effects on saturated pool boiling heat transfer from superheated horizontal surfaces having multi-cavities of rectangular shapes under constant wall temperature conditions are investigated numerically by a liquid–vapor phase-change lattice Boltzmann method. It is shown that mutual suppression of bubble nucleation between cavities exists, and this effect depends not only on pitch distance of cavities but also on the depth/width and location of the cavities as well. For cavities with unequal sizes, bubbles tend to nucleate preferentially in wider or deeper cavities while bubble nucleation in narrow or shallow cavities can be totally suppressed at small pitch distances. Saturated pool boiling curves, from natural convection regime to stable film boiling regime on a *hydrophilic* rough surface, a *hydrophobic* rough surface as well as a *mixed* wettability rough surface (a *hydrophilic* surface having *hydrophobic* cavities) are obtained numerically. Simulated results show that presence of roughness on the heating surface promotes boiling incipience and enhances boiling heat flux in the nucleate boiling regime. A more pronounced enhancement of the nucleate boiling heat transfer is observed on a *hydrophobic* rough surface than that on a *hydrophilic* rough surface at the same wall superheat. Among three types of rough surfaces, the mixed wettability rough surface (with *hydrophobic* cavities on a *hydrophilic* surface) exhibits the best overall boiling heat transfer performance with higher boiling heat flux in the nucleate boiling regime than the *hydrophilic* rough surface and the highest critical heat flux.

1. Introduction

Although roughness effects have been recognized to play an important role in boiling heat transfer in early years [1–3], a systematic research on roughness effects in boiling did not begin until the 21st century owing to advances in microfabrication technologies [4,5]. In recent years, an extensive amount of experiments [6–10] has been conducted to study roughness effects on pool boiling heat transfer performances in terms of boiling incipience, heat transfer coefficient as well as critical heat flux (CHF). In particular, Wei and Honda [6] studied pool boiling heat transfer on silicon chips with square micro-pin-fins and demonstrated that micro-pin-fins could effectively enhance boiling heat transfer coefficients in nucleate boiling regime and the critical heat flux. It was also shown that the critical heat flux would increase monotonically with increasing micro-pin-fin height for a fixed value of the micro-pin-fin thickness. Yu and Lu [7] investigated saturated pool boiling of FC-72 on copper surfaces with rectangular fin arrays. They found that boiling generally initiated at the tip of the fin and boiling heat transfer enhancement was lower for low superheats than that for high superheats. Dong et al. [10] conducted pool boiling experiments on rough surfaces with micro- and nano-sized structures, and showed that microstructures could significantly increase the active nucleation site density at low heat fluxes while nano-structures could delay bubble mergence and formation of vapor films at high heat fluxes during boiling crisis.

Nucleation site interactions, which typically exist on rough boiling surfaces with multiple cavities, have been found to play important roles on pool boiling heat transfer performances [11–19]. Gjerkeš and Golobič [15] experimentally studied effects of the distance between nucleation sites on their mutual interactions, and showed that deactivation of a weaker, less-active nucleation site may occur at very small distances between nucleation sites. To illustrate physical mechanisms of nucleation site interactions in pool boiling, Zhang and Shoji [16] conducted experiments on a thin silicon surface having two artificial cavities. Coexistence and competition of three factors, i.e., the hydrodynamic interaction between bubbles, the thermal interaction between nucleation sites and horizontal and declining bubble coalescences, were found at different cavity pitch distances.

* Corresponding author.
E-mail address: pingcheng@sjtu.edu.cn (P. Cheng).

http://dx.doi.org/10.1016/j.ijheatmasstransfer.2016.04.082
0017-9310/

Nomenclature

$c_{p,l}$	specific heat of the liquid (J kg^{-1} K^{-1})
h_{fg}	latent heat (J/kg)
H	thickness of the heater (m)
H^*	dimensionless thickness of the heater
H_{ca}	cavity height (m)
H^*_{ca}	dimensionless cavity height
Ja	Jacob number
l_0	capillary length (m)
L_h	heater size (m)
$L_h{}^*$	dimensionless heater size
L_x	length of the computation domain in x direction (m)
L_y	length of the computation domain in y direction (m)
$\mathbf{n}$	unit vector normal to the boundary of the rough surface
P	pitch distance between adjacent cavities (m)
P^*	dimensionless pitch distance between adjacent cavities
$q(x, t)$	local heat flux (W/m^2)
$\bar{q}(x, t)$	dimensionless local heat flux
$\bar{q}'(t)$	dimensionless space-averaged heat flux
$\bar{q}''$	dimensionless space- and time-averaged heat flux
t	time (s)
t^*	dimensionless time
t_0	characteristic time (s)
T	temperature (K)
T'	dimensionless temperature
u_0	characteristic velocity (m/s)
W_{ca}	cavity width (m)
W^*_{ca}	dimensionless cavity width
x	co-ordinates (m)
y	co-ordinates (m)

Greek symbols

θ	static contact angle (°)
λ	thermal conductivity of the heated plate (W m^{-1} K^{-1})
σ	surface tension (N/m)
δ	lattice spacing (m)
∇	gradient operator

Subscripts or superscripts

c	critical
l	liquid
s	saturation
v	vapor
w	wall

Relatively few papers have been published on analytical or numerical studies on roughness effects on boiling heat transfer [20,21]. Dong et al. [22] performed a thermodynamic analysis on onset of bubble nucleation on a rough superheated surface in pool boiling. Quan et al. [23] proposed a critical heat flux model for rough surfaces. In Part I of this paper series [24], nucleation, growth and departure of a bubble from a single cavity on a surface with uniform wettability or with mixed wettability in pool boiling at low superheats have been numerically studied. Numerical investigation on nucleation site interactions on rough surfaces having multi-cavities is presented in Part II of this paper series here. Saturated pool boiling curves on rough surfaces are obtained by numerical simulation for the first time and roughness effects on saturated pool boiling curves are obtained. Some preliminary simulation results on bubble interactions above multi-cavities on superheated surfaces in pool boiling were briefly discussed recently in two review papers [20,21].

2. Results and discussion

In this paper, we will use Gong–Cheng liquid–vapor phase change lattice Boltzmann model [25–27] to study roughness effects on saturated pool boiling heat transfer from superheated horizontal surfaces with multi-cavities. Since the model has been reviewed in Part I of this paper series, we will not repeat its presentation here.

2.1. Computation setup

As shown in Fig. 1, a heated horizontal plate (indicated in red) with a length L_h and thickness H is located at the central part of the bottom wall. Multiple cavities (with a pitch distance P, cavity width W_{ca} and cavity depth H_{ca}) acting as nucleation sites are located at the top of the heater. Following Part I of this paper series [24], the characteristic length l_0, the characteristic velocity u_0 and the characteristic time t_0 are chosen as [28]:

$$l_0 = \sqrt{\frac{\sigma}{g(\rho_l - \rho_v)}}, \quad u_0 = \sqrt{g l_0}, \quad t_0 = l_0/u_0 \qquad (1a, 1b, 1c)$$

where l_0 is the "capillary length" representing the ratio of surface tension and buoyancy force.

As in Part I of this paper series, the computation domain is a 600×600 lattice region (corresponding to $L_x \times L_y = 33.8 l_0 \times 33.8 l_0$). The heater size is $L_h = 11.3 l_0$ in length with a thickness $H = 1.1 l_0$, where a conjugate heat transfer problem including heat conduction in the heated plate is considered here. Constant wall temperature (T_w) boundary condition (expressed in terms of the Jakob number $Ja = c_{p,l}(T_w - T_s)/h_{fg}$) is specified on the bottom of the heated plate (at $y = 0$) and the left and right sides of the heated plate are adiabatic. Periodic boundary conditions and the convective boundary condition are imposed on left/right sides and top of the computation domain, respectively. Initially, the computation domain is occupied by motionless saturated water at $T_s = 0.9T_c$ (corresponding to a saturated liquid/vapor density ratio of 10), and the whole pool boiling process including bubble nucleation on the rough heating surface is simulated after the wall temperature is imposed. Table 1 is a list of dimensionless parameters (where $P^* = P/l_0$, $W^*_{ca} = W_{ca}/l_0$ and $H^*_{ca} = H_{ca}/l_0$) used for

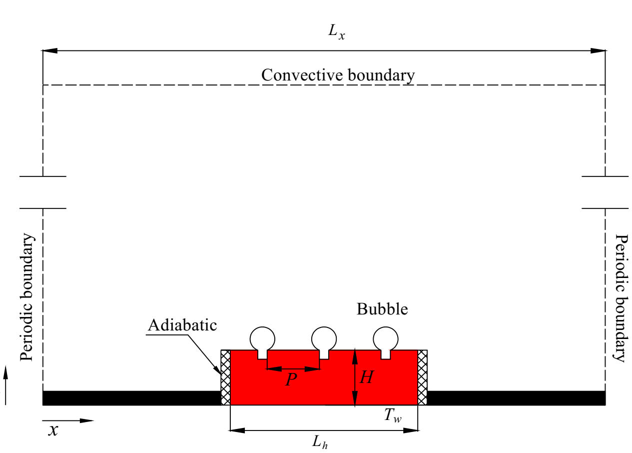

Fig. 1. Schematic of the computation domain. (For interpretation of the references to colour in this figure legend, the reader is referred to the web version of this article.)